HHS Public Access

Author manuscript

Oncogene. Author manuscript; available in PMC 2016 March 05.

Published in final edited form as:

Oncogene. 2015 March 5; 34(10): 1312–1322. doi:10.1038/onc.2014.63.

Tumor-Derived Inducible Heat Shock Protein 70 (HSP70) is an Essential Component of Anti-Tumor Immunity

Keela Dodd[1], **Stephanie Nance**[1], **Melanie Quezada**[1], **Laura Janke**[2], **Jeffrey B Morrison**[3], **Richard T Williams**[3,4], and **Helen M Beere**[1,*]

[1]Department of Immunology, St Jude Children's Research Hospital, 262 Danny Thomas Place, Memphis, TN, 38105, USA

[2]Veterinary Pathology Core, St Jude Children's Research Hospital, 262 Danny Thomas Place, Memphis, TN, 38105, USA

[3]Department of Oncology, St Jude Children's Research Hospital, 262 Danny Thomas Place, Memphis, TN, 38105, USA

[4]PUMA Biotechnology, 10880 Wilshire Blvd, Suite 2150, LA, CA, 90024, USA

Abstract

The anti-apoptotic function and tumor-associated expression of HSP70 is consistent with HSP70 functioning as a survival factor to promote tumorigenesis. However, its immunomodulatory activities to induce anti tumor immunity predict the suppression of tumor growth. Using the *Hsp70.1/3*$^{-/-}$ (*Hsp70*$^{-/-}$) mouse model, we observed that tumor-derived HSP70 was neither required for cellular transformation nor for *in vivo* tumor growth. *Hsp70*$^{-/-}$ murine embryonic fibroblasts (MEFs) were transformed by *E1A/Ras* and generated tumors in immune deficient hosts as efficiently as WT transformants. Comparison of *Bcr-Abl*-mediated transformation of WT and *Hsp70*$^{-/-}$ bone marrow and progression of B cell leukemogenesis *in vivo* revealed no differences in disease onset or survival rates and *Eμ-Myc* driven lymphoma in *Hsp70*$^{-/-}$ mice was phenotypically indistinguishable from WT *Eμ-Myc* mice. However, *Hsp70*$^{-/-}$ *E1A/Ras* MEFs generated significantly larger tumors than their WT counterparts in C57BL/6J immune competent hosts. Concurrent with this was a reduction in intra-tumoral infiltration of innate and adaptive immune cells, including macrophages and CD8^{+} T cells. Evaluation of several potential mechanisms revealed an HSP70-chemokine-like activity to promote cellular migration. These observations support a role for tumor-derived HSP70 in facilitating anti-tumor immunity to limit tumor growth and highlight the potential consequences of anti-HSP70 therapy as an efficacious anti-cancer strategy.

Keywords

HSP70; anti-tumor immunity; intra-tumoral lymphocytes

[*]**Corresponding Author:**helen.beere@stjude.org; 901-595-4975 (telephone).

Conflict of Interest: All authors declare no potential conflicts of interest

INTRODUCTION

Heat shock proteins (HSPs), the functional components of the inducible heat shock response are implicated in the regulation of tumorigenesis by virtue of their ability to promote tumor cell survival (Ciocca et al 2013). However, the only *in vivo* genetic evidence of a pro-tumorigenic role for the stress response is the abrogation of tumor formation in mice deficient for heat shock factor-1 (HSF-1), the transcription factor essential for the expression of multiple HSPs (Dai et al 2007, Min et al 2007). Nevertheless, evidence suggests that 'addiction' to components of the stress response, including HSP70, may sustain tumor survival and drive tumor growth (Ciocca et al 2013, Rohde et al 2005).

HSP70 also regulates immune function, including antigen cross presentation (Binder and Srivastava 2005, Li et al 2002), dendritic cell maturation (Srivastava 2002a, Srivastava 2002b) and NK cell (Elsner et al 2007, Gross et al 2003) and MDSC (Chalmin et al 2010) activities. Extracellular HSP70 regulates these diverse immunoregulatory activities by acting as a cytokine to stimulate the release of pro-inflammatory factors from immune cells (Asea et al 2000) or from tumor cells (Chen et al 2009). HSP70 is released from tumor cells via passive release from dying cells and active trafficking via the endolysosomal pathway (Mambula and Calderwood 2006) or release within lipid bound exosomes (Chalmin et al 2010, Vega et al 2008).

Discrimination between a need for tolerance and the demand for immunity represents a fundamental principal of maintaining immunological homeostasis. Tolerance prevents autoimmunity, but because of the extensive overlap of self-peptides with tumor-associated antigens, also suppresses anti-tumor immunity. The immune system can distinguish 'normal' from 'abnormal' self to overcome tolerance and instead invoke immunity via mechanisms such as the release of immunogenic 'danger signals' (Matzinger 1994), that include HSPs (Borges et al 2012, van Eden et al 2012). Although HSPs may be critical determinants of a need for tolerance or circumstances requiring an immune response (Kottke et al 2009, Millar et al 2003), it remains controversial if this is mediated by promoting immunity or by suppressing immune responses to maintain tolerance (Stocki and Dickinson 2012, van Eden et al 2012).

To date, no studies have utilized the *Hsp70.1/3*$^{-/-}$ murine model, to address if HSP70, like HSF-1 (Dai et al 2007, Min et al 2007), is a critical pro-survival signal for tumor cells *in vivo* or to evaluate the consequences of HSP70-mediated immune regulation in the context of anti-tumor immunity and tumor growth *in situ*. Clearly, HSP70 can contribute to multiple aspects of immune regulation, but it remains unclear if this manifests in the suppression of tumor growth by activation of anti-tumor immunity (Blachere et al 1997, Udono and Srivastava 1993 or immunosuppression to exacerbate tumorigenesis (Stocki and Dickinson 2012).

We utilized the *Hsp70.1/.3*$^{-/-}$ murine model, in which both alleles of inducible HSP70 are deleted (Hunt et al 2004), to ask if HSP70 is essential for oncogene-induced transformation; if HSP70 plays a non-redundant role in tumor growth *in vivo*; if the immunoregulatory activity of HSP70 inhibits or promotes tumor growth *in vivo*? We present data here that

challenge an essential pro-tumorigenic role for tumor derived HSP70 but instead support a model in which it *negatively* regulates tumor growth *in vivo* by engaging T cell dependent immunity. For the first time, using the *Hsp70.1.3*$^{-/-}$ murine model, we demonstrate that HSP70 is a non-essential pro-tumorigenic factor but instead functions as a danger signal to facilitate anti-tumor immunity and suppress tumor growth *in vivo*.

MATERIALS AND METHODS

Additional details are included in Supplementary Information.

Animals

All mice were cared for in accordance with NIH guidelines and adhering to procedures approved by St Jude Children's Research Hospital Animal Care and Use Committee (IACUC). Genotyping was conducted according to published methods (Hunt et al 2004) and online at jaxmice.jax.org.

Preparation, *In Vitro* Transformation and Maintenance of Mouse Embryo Fibroblasts (MEFs)

Timed heterozygous breeding between appropriate genotypes was used to generate embryos WT or null for *HSF-1* or *Hsp70*. Retroviral particles were produced using the ecotropic Phoenix packaging cell line with the following plasmids: pWZL-hygro; pBABE-puro; pWZL-hygro 12S *E1A* or pBABE-puro *K-Ras* V12 (purchased from Addgene, Cambridge, MA). Primary WT or *Hsp70*$^{-/-}$ MEFs were infected with virus for 6h before medium replacement, antibiotic selection and colony outgrowth visualized by methylene blue staining. In some experiments, transformed MEFs were maintained in culture for experimentation – the genotype was confirmed by qPCR and cell lines were maintained *in vitro* for a maximum of 10 passages before rescue of an earlier passage from liquid nitrogen storage. All cell lines generated were tested approximately every 3 months for mycoplasma contamination using MycoSEQ™ Mycoplasma Detection Assay (In Vitrogen) and discarded if found to be positive.

MEF Tumor Implantation

WT or *Hsp70*$^{-/-}$ *E1A/Ras* MEF transformants were introduced subcutaneously into each of the flanks of CD1-*Foxn1*^{nu}, C57BL/6J or *Hsp70*$^{-/-}$ and tumor growth monitored via ultrasound imaging. Tumor volumes were calculated using the VEVO-770 software (version 3.0.0) and once tumor volume reached 20% of body mass, mice were euthanized and tumor tissue harvested for subsequent analyses by flow cytometry.

Plasmids Used/Transfections/Transductions

WT transformants stably expressing HuSH pRFP-c-RS shRNAs for *Hspa1a* and *Hspa1b* or the shRNA pRFP-c-RS negative control (all purchased from OriGene, Rockville, MD) were generated. A retroviral vector encoding p185 Bcr-Abl and GFP (MSCV-IRES-GFP) was used to generate retroviral particles by transfection of Phoenix-Eco cells (Invitrogen).

RNA isolation and qPCR

Total RNA was used to generate cDNA and quantitative PCR performed using a 7900HT Fast Real time PCR system (Applied Biosystems, Foster City, CA) using standard conditions for Sybr Green PCR Master Mix (ABI).

Histopathology and Immunohistochemistry

Tumors were first fixed in 4% PFA overnight. Those used for paraffin sections were transferred to 10% neutral buffered formalin and embedded in paraffin wax, 4μM sections were prepared, stained with H&E and examined microscopically. Tumors used for cryosections were washed with PBS after overnight fixation and placed in 30% sucrose at 4°C before transfer into OCT embedding compound.

Confocal Images

Confocal images were taken using a Zeiss LSM 510 NLO Meta point scanning confocal/ multiphoton microscope and Zen software.

Immunoblot

WT *E1A/Ras* MEFs stably expressing *Hspa1a/Hspa1b* or negative control RFP-shRNAs were subjected to heat shock for one hour at 42°C before recovery at 37°C for two hours. Extracts were prepared and analyzed by immunoblotting for HSP70/HSP72 (1:1000; Enzo Life Sciences), RFP (1:2000; Origene) and actin (1:400; MP Biomedicals, Solon, OH).

Culture of *Bcr-Abl*-Transduced Bone Marrow

Procedures were performed as described previously (Williams et al 2006). WT or $Hsp70^{-/-}$ bone marrow was transduced with *Bcr-Abl-GFP* and cells maintained in culture or introduced into lethally irradiated WT recipients.

Eμ-Myc Model of Lymphomagenesis

Cohorts of *Eμ-Myc* mice, WT, heterozygous and null for *Hsp70* were monitored for onset of disease (Adams et al 1985). Lymphoid organs were harvested for subsequent analysis via immunostaining and flow cytometric analysis.

Migration Assays

Migration assays were conducted using the ChemoTx system (Neuro Probe, Inc., Gaithersburg, MD). Splenocytes isolated from mice inoculated with WT or $Hsp70^{-/-}$ *E1A/Ras* MEF transformants 5 days prior, were introduced into the upper chamber above WT or $Hsp70^{-/-}$ MEF transformants and after a 4 hour incubation at 37°C, the cell number in the lower well was enumerated using a Scepter cell counter (EMD Millipore, Billerica, MA).

Antigen Cross Presentation

Hsp70.1/.3$^{-/-}$ or WT bone marrow was maintained in culture with 20ng/ml recombinant murine GM-CSF (Peprotech, Rocky Hill, NJ). After 7 days enriched DCs (10^5) were cultured overnight without GM-CSF before addition of Class I OVA peptide 257–264

(100μM). The following day OT-I transgenic T cells added to the wells and cells counted after 72h.

Statistical Analysis

Statistical significance was determined according to the test described in the relevant figure legend.

RESULTS

HSP70 is Neither Required for Oncogene-Induced Transformation *in vitro* nor Tumor Growth *in vivo*

WT or *Hsp70*$^{-/-}$ MEFs transduced with *E1A* and *Ras*, but not empty vector or *E1A* or *Ras* alone, generated drug resistant colonies after approximately 2 weeks. In contrast, but consistent with observations using immortalized *HSF-1*$^{-/-}$ MEFs (Dai et al 2007), primary *HSF-1*$^{-/-}$ MEFs did not transform (Figure 1A). qPCR of *Hsp70* expression confirmed the genotype of emergent clones (Figure 1B). WT and *Hsp70*$^{-/-}$ *E1A/Ras* transformants generated tumors in immunodeficient mice with no significant difference in tumor size (Figures 1C and 1D). Similar data were obtained using independently generated WT and *Hsp70*$^{-/-}$ *E1A/Ras* transformants. All tumors were classified as sarcomas (Supplementary Figures 1A–B) and neither the frequency of karyomegaly nor mitoses revealed any significant difference between WT and *Hsp70*$^{-/-}$ tumors (Supplementary Figure 1C).

Selection for HSP70 Expression in WT Tumors

WT tumors from CD1-*Foxn1*^{nu} mice had elevated *Hsp70* gene expression, compared to the MEFs used for inoculation (Figure 1E). *Hsp70*$^{-/-}$ tumors were not completely devoid of *Hsp70* expression, presumably due to host-derived contamination (Figure 1E) and *Hsp90AA1* gene expression in WT and *Hsp70*$^{-/-}$ tumors was comparable and largely unchanged from that in the MEFs used for inoculation (Figure 1F).

Neither *Bcr-Abl* nor *Eμ-Myc* requires HSP70 to Induce Leukemogenesis

We also examined the requirement for HSP70 in i) *Bcr-Abl*-induced leukemogenesis (Williams et al 2006) and ii) *Eμ-Myc*-induced B cell lymphoma (Adams et al 1985). WT and *Hsp70*$^{-/-}$ bone marrow (BM) was transduced with a retroviral vector expressing *Bcr-Abl-GFP* before culture *in vitro* or transfer into lethally irradiated C57BL/6J WT hosts. WT and *Hsp70*$^{-/-}$ BM cultures proliferated at similar rates before (Figure 2A) and after (Figure 2B) removal from stromal support. Equivalent GFP expression was detected in the WT and *Hsp70*$^{-/-}$ BM transformants (Figure 2C) and evaluation of *Hsp70* confirmed genotype specificity (Figure 2D). Similar disease onset was observed in animals receiving WT or *Hsp70*$^{-/-}$ bone marrow, with no significant difference in overall survival rates (Figure 2E). No genotype-specific differences were observed in spleen weight (Figure 2F) or % GFP positivity, a surrogate determinant of *Bcr-Abl*$^{+}$ cells (Figure 2G).

Eμ-Myc transgenic mice (Adams et al 1985), WT, heterozygous or null for *Hsp70* developed disease with a similar time of onset (Figure 2H), spleen weight (Figure 2J) and disease classification (Figure 2K). However, while the median survival rate of WT and *Hsp70*$^{+/-}$-

Eμ-Myc mice was similar, *Hsp70*$^{-/-}$ mice exhibited a significant increase in lifespan (Figures 2H and 2I).

Tumor-Derived HSP70 Only Retards Tumor Growth in an Immune Competent Host

To specifically address the role of intra-tumoral HSP70, we further utilized the MEF-derived sarcoma model. WT *E1A/Ras* cells introduced into immune competent hosts formed small tumors that subsequently regressed, while *Hsp70*$^{-/-}$ transformants generated significantly larger tumors (Figures 3A and 3B). This contrasts with equivalent WT and *Hsp70*$^{-/-}$ tumor growth in immunodeficient hosts (Figures 3C and 1C). WT tumors generated in C57BL/6J hosts showed increased *Hsp70* gene expression compared to the cells used for inoculation (Figure 3E), although the average fold difference was less than in the CD1-*Foxn1*^{nu} mice (compare Figures 3E and 1E). Immunohistochemistry confirmed HSP70 expression in WT tumors that was largely absent from *Hsp70*$^{-/-}$ tumors (Figure 3D and Supplementary Figures 1F–G). *Hsp90AA1* expression was increased in *Hsp70*$^{-/-}$ but not WT tumors (Figure 3F) and constitutive *Hsc70* remained at or below control levels in WT and *Hsp70*$^{-/-}$ tumors (Figure 3G).

Hsp70$^{-/-}$ Tumors Display a Marked Reduction in the Infiltration of Immune Cells

WT tumors from C57BL/6J hosts displayed macrophage infiltration throughout the tumor mass while those lacking *Hsp70*, showed a reduction in MAC-2 staining that was largely restricted to the tumor periphery (Figure 4A and Supplementary Figures 2C–2D). Although *Hsp70*$^{-/-}$ tumors from CD1-*Foxn1*^{nu} hosts also showed a reduction in macrophage number compared to WT tumors, they were distributed throughout the tumor mass (Figure 4B and Supplementary Figures 2A–B).

Differential growth of WT and *Hsp70*$^{-/-}$ tumors in C57BL/6J hosts compared to equivalent growth in CD1-*Foxn1*^{nu} mice suggests that HSP70 may suppress tumor growth in a T cell dependent manner. Indeed, WT tumors displayed extensive intra-tumoral lymphocytic infiltration while *Hsp70*$^{-/-}$ tumors were characterized by a reduced number of CD3^{+} cells, largely restricted to the tumor periphery (Figure 4C and Supplementary Figure 3). Extensive intra-tumoral CD3^{+}/CD4^{+} (Figure 5A) and CD8^{+}/GrB^{+} (Figure 5B) co-staining was observed in WT tumors that was reduced and largely undetectable in *Hsp70*$^{-/-}$ tumors. NKT cells were detected in WT and, to a lesser extent, *Hsp70*$^{-/-}$ tumors (Figure 5C) and while WT tumors had extensive granzyme B and perforin expression, *Hsp70*$^{-/-}$ tumors exhibited a reduction in the expression of both (Figures 5D–5E and Supplementary Figures 4D–4G).

Knockdown of *Hsp70* Abrogates Intra-Tumoral Immune Cell Infiltration and Promotes Tumor Growth

WT MEFs stably expressing *Hsp70* or control shRNAs vectors co-expressing RFP were evaluated for their ability to generate tumors *in vivo*. *Hsp70* shRNAs reduced HSP70 protein levels while RFP expression was equivalent in both control and *Hsp70* shRNA expressing cells (Figure 6A and Supplementary Figures 5A–B). Tumors expressing *Hsp70* or control shRNAs were equal in size in immunodeficient mice (Figure 6B) but in C57BL/6J hosts, cells expressing *Hsp70* shRNA generated larger tumors compared to those expressing

control shRNAs (Figure 6D). Furthermore, *Hsp70* shRNA tumors from immune competent mice displayed a selective retention of RFP and reduced HSP70 proteins (Figures 6E and Supplementary Figures 5I–L). In contrast, RFP protein levels were variable in tumors isolated from CD1-*Foxn1*^{nu} hosts with no preferential expression in the *Hsp70*$^{-/-}$ tumors (Figure 6C and Supplementary Figures 5C–H). *Hsp70* shRNAs expressing tumors displayed a marked reduction in macrophage and T cell infiltration as compared to control shRNA tumors (Figures 6F and 6H and Supplementary Figures 5M and 5N respectively). In contrast, macrophage distribution was indistinguishable between WT and *Hsp70*$^{-/-}$ tumors harvested from CD1-*Foxn1*^{nu} hosts (Figures 6G and Supplementary Figure 5O). These data confirm that tumor growth *in vivo* is inhibited by *Hsp70*-dependent immunoregulation that paradoxically, is opposed by an immune-dependent selection against HSP70 expression (Figure 6E).

Tumor-Derived HSP70 Functions in a Chemokine-Like Manner to Facilitate Intra-Tumoral Infiltration of Immune Cells

HSP70 can augment antigen cross presentation (Srivastava 2002a, Srivastava 2002b), consistent with suppression of T cell activation and exacerbation of tumor growth observed in our *Hsp70*$^{-/-}$ model. However, bone marrow derived dendritic cells (BMDCs), were equally capable of cross-presenting irradiated WT and *Hsp70*$^{-/-}$ MEFs preloaded with Class I MHC SIINFEKL peptide as determined via transgenic OT-I CD8^{+} T cell proliferation (Supplementary Figure 6A). Evaluation of the number and activity of NK and NKT cells found neither to be lacking in WT hosts harboring *Hsp70*$^{-/-}$ tumors (Supplementary Figure 6B) and characterization of phenotypic and functional features shared by tumor associated macrophages and myeloid derived suppressor cells (MDSCs), both of which can augment tumor growth, revealed no difference in frequency or distribution as compared to MAC-2 staining (Supplementary Figures 6C and 6D). Therefore, three modes of immune activity that can be regulated by HSP70 could not account for the exacerbation of *Hsp70*$^{-/-}$ tumor growth that we observed.

WT or *Hsp70*$^{-/-}$ *E1A/Ras* transformants were each introduced into cohorts of WT and *Hsp70*$^{-/-}$ C57BL/6J hosts and tumor growth monitored. WT MEFs generated significantly smaller tumors compared to their *Hsp70*$^{-/-}$ counterparts regardless of the host genotype and the exacerbated growth of *Hsp70*$^{-/-}$ tumors in WT mice was also observed in *Hsp70*$^{-/-}$ hosts (Figure 7A). Furthermore, the reduction in WT tumors in either WT or *Hsp70*$^{-/-}$ hosts correlated with a pronounced infiltration of immune cells while the larger *Hsp70*$^{-/-}$ tumors were instead characterized by a largely peripheral and minimal intra-tumoral distribution of macrophages and T cells in both WT and *Hsp70*$^{-/-}$ hosts (Figures 7B and 7C respectively). We conclude that tumor derived HSP70 is impacting tumor growth independent of intrinsic tumor cell survival but by regulating immune cell infiltration in a localized manner.

Splenocytes from WT C57BL/6J mice inoculated 5–7 days prior with WT or *Hsp70*$^{-/-}$ MEFs, were co-cultured with WT or *Hsp70*$^{-/-}$ *E1A/Ras* MEFs and after 4 hours, the number of splenocytes in the lower chambers enumerated. WT splenocytes primed in a host harboring a WT tumor migrated at a frequency proportional to the number of WT MEFs plated in the lower chamber (Figure 7D). In comparison, the migration of WT splenocytes

primed *in vivo* by *Hsp70*$^{-/-}$ MEFs, occurred at significantly reduced numbers that inversely correlated with the number of *Hsp70*$^{-/-}$ MEFs (Figure 7D). Strikingly, WT splenocytes primed by WT tumors failed to migrate towards *Hsp70*$^{-/-}$ MEFs and in the reciprocal scenario, WT splenocytes primed by *Hsp70*$^{-/-}$ tumors were not stimulated to migrate by WT MEFs (Figure 7D). Importantly, naïve splenocytes with no prior *in vivo* priming, migrated towards WT and *Hsp70*$^{-/-}$ MEFs in equivalent numbers (Figure 7E). These observations are consistent with the idea that tumor-derived HSP70 can function as a chemokine within the localized tumor microenvironment to facilitate intra-tumoral immune cell infiltration.

DISCUSSION

We have found that, remarkably, both alleles of inducible HSP70 were dispensable for oncogenesis and tumor growth in three models of transformation. Further, while the absence of HSP70 was irrelevant for growth of transformed MEF in immunocompromised hosts, it resulted in defective immunity and enhanced tumor growth in immunocompetent animals. These studies are the first to utilize a genetically defined model and allowed us to isolate the requirement for HSP70 as an endogenous factor to sustain tumor cell survival and its extra-tumoral role to modulate the host immune response. Clearly HSP70 *can* sustain tumor survival and regulate immune function, but we suggest that in those cases where HSP70 is dispensable for oncogenesis it may instead contribute to anti-tumor immunity. Understanding the mechanisms through which HSP70 can regulate tumorigenesis *in situ* is critical if efforts to exploit the stress pathway as an anti-cancer strategy are to succeed (Leu et al 2009).

HSP70 is neither required for oncogene-driven transformation nor for tumor growth *in vivo* in three independent *in vivo* models (Figures 1–2) and opposes the idea that tumor derived HSP70 is absolutely necessary for tumor cell survival. It is possible however, that WT tumors acquire a dependency for HSP70 expression, whereby its disruption could provoke tumor cell death (Nylandsted et al 2000). However, *E1A/Ras* transformants stably expressing *Hsp70* shRNAs formed tumors *in vivo* (Figures 6B and 6D), implying that cells transformed in the *presence* of HSP70 not only survive but remain tumorigenic. While our data are unanimous regarding a non-critical role for HSP70 in tumor generation, we did observe an increase in the mean survival of *Eμ-Myc- Hsp70*$^{-/-}$ mice (Figures 2H–I), suggesting that, at least in this model, HSP70 may provide a tumor intrinsic survival signal. However, it is also possible that the lack of *Hsp70* expression in a non-tumor tissue contributed to this phenotype.

The selection for *Hsp70* expression in WT tumors (Figure 1E) implies that its retention may be advantageous, either to the tumor or to the host. *Hsp70*$^{-/-}$ tumors were significantly larger than their WT counterparts in C57BL/6J hosts (Figure 3A), as compared to their equivalent growth in immune deficient hosts (Figures 1C and 3C). *Hsp70*$^{-/-}$ tumors were characterized by reduced intra-tumoral immune infiltrate (Figures 4 and 5), suggesting that tumor-derived HSP70 can influence the recruitment, retention or activation of anti-tumor immune cells.

Although HSP70 can promote the activity of NK cells (Multhoff 2002), we observed no decrease in *Hsp70*$^{-/-}$ tumors (Figure 5). In addition, both NK (CD3^{-} NK1.1^{+}) and NKT (CD3^{+} NK1.1^{+}) cell numbers and activity was increased in mice harboring *Hsp70*$^{-/-}$ tumors (Supplementary Figure 7B). While the reason for this is unclear, it cannot explain the increased growth of *Hsp70*$^{-/-}$ tumors, but is consistent with HSP70 mediating immune suppression under some circumstances (Stocki and Dickinson 2012, Stocki et al 2012). Quantification of T cells in tumor bearing mice did not reveal preferential accumulation of any sub-type based on the HSP70 status of the tumor. Interestingly however, while the CD3^{+} population appeared largely confined to the periphery of *Hsp70*$^{-/-}$ tumors, FoxP3^{+} cells were distributed throughout (Supplementary Figures 4A–B). HSP70 can enhance the immunosuppressive activity of FOXP3^{+} T_{regs} (van Herwijnen et al 2012, Wachstein et al 2012) and although we cannot exclude this possibility, it is inconsistent with enhanced *Hsp70*$^{-/-}$ tumor growth. Analysis of tumor associated macrophages (TAMs) and myeloid derived suppressor cells (MDSCs) (Chalmin et al 2010), also failed to reveal any skewing of distribution or number in *Hsp70*$^{-/-}$ tumors or in mice harboring them (Supplementary Figures 7C and 7D).

While WT tumors were characterized by an increase in *Hsp70* expression (Figures 1E and 3E), those expressing *Hsp70* shRNAs displayed a preferential retention of high RFP and reduced HSP70 expression (Figure 6 and Supplementary Figure 5). Cancer immunoediting incorporates the ‘surveillance’ aspect of immune function to prevent tumor formation and the detrimental selection for tumor variants with reduced immunogenicity capable of evading host immune pressure (Dunn et al 2004, DuPage et al 2012). It is therefore intriguing to speculate that the T cell-dependent selective deletion of tumor cells expressing the highest HSP70 levels nominates HSP70 as a determinant of the immunoediting process. Therefore, the selection for HSP70 sustains tumor immunogenicity, vulnerability to lymphocyte attack and tumor cell deletion. Consistent with this, HSP70 tumor content decreases as tumors advance and high HSP70 levels provide a prognostic indicator of survival (Effendi and Sakamoto 2010, Malusecka et al 2008, Torronteguy et al 2006).

HSP70 (Blachere et al 1997, Li et al 2002) (Zietara et al 2009) facilitates antigen cross presentation to engage CD8^{+}-dependent cytolytic activity. However, BMDCs were equally capable of cross presenting antigens from WT and *Hsp70*$^{-/-}$ *E1A/Ras* transformants (Supplementary Figure 7A) and reciprocal implantation of WT or *Hsp70*$^{-/-}$ tumor cells into *Hsp70*$^{-/-}$ or WT hosts respectively, produced tumors and immune infiltration indistinguishable from their growth in hosts of the same genotype (Figures 7A–C). Collectively, these data are inconsistent with HSP70 within the tumor itself or in peripheral APCs facilitating antigen cross presentation.

Extracellular HSP70 can regulate immune cells (Chalmin et al 2010, Mambula and Calderwood 2006, Multhoff 2002) to suppress tumor growth (Daniels et al 2004, Kottke et al 2009). Splenocytes pre-primed *in vivo* by WT tumors migrated towards WT transformants, while those pre-primed by *Hsp70*$^{-/-}$ tumors were unable to migrate towards *Hsp70*$^{-/-}$ tumor cells (Figure 7D). The dependence of splenocyte migration upon pre-priming (Figure 7E) suggests that HSP70 imparts migratory activity to immune cells within the tumor microenvironment. Inhibition of the migratory capacity of splenocytes from mice

harboring WT tumors by co-culture with *Hsp70*$^{-/-}$ splenocytes (Figure 7D) suggests that *Hsp70*$^{-/-}$ tumor cells are deficient in a stimulatory factor that functions either directly or indirectly.

Using the *Hsp70.1/.3*$^{-/-}$ model we demonstrate a non-critical tumor intrinsic role for HSP70 in tumor growth *in vivo*. Instead, HSP70 represents a critical component for tumor recognition by the adaptive immune system and promotes host immunity *in situ* to promote tumor destruction.

MATERIALS AND METHODS

Animals

Hsp70$^{-/-}$ mice were derived as previously described (Hunt et al. 2004), backcrossed at least 6 times to C57BL/6J mice and maintained as heterozygous breeding pairs. Immunocompromised athymic mice (CD1-*Foxn1*^{nu}) (Charles River Laboratories, Wilmington, MA) or C57BL/6J (Jackson Laboratories, Bar Harbor, ME) were used as allograft recipients in the *in vivo* tumor studies. *Eμ-Myc*-C57BL/6J lymphoma-prone mice were obtained from Dr John Cleveland, Scripps Research Institute, Jupiter, FL) (Adams et al. 1985) and crossed with the *Hsp70*$^{+/-}$-C57BL/6J strain to generate *Eμ-Myc* transgenic positive mice, WT, heterozygous or null for *Hsp70*. OT-I transgenic mice were purchased from Jackson Laboratories when needed. All mice were cared for in accordance with NIH guidelines and adhering to procedures approved by St Jude Children's Research Hospital Animal Care and Use Committee (IACUC). Genotyping was conducted according to published methods (Hunt et al. 2004) and online at jaxmice.jax.org.

Preparation, *In Vitro* Transformation and Maintenance of Mouse Embryo Fibroblasts (MEFs)

Timed heterozygous breeding between appropriate genotypes that was verified by ultrasound imaging was used to generate embryos WT or null for *HSF-1* or *Hsp70*. At day 10–12 embryos were harvested for genotyping and isolation of MEFs via enzymatic digestion. MEFs were grown in DMEM, 10% FBS, 2mM nonessential amino acids, 100U/ml penicillin/streptomycin, 2mM glutamine and 0.5% β-mercaptoethanol to 80–90% confluence and used for up to approximately 5 passages before the onset of senescence.

Retroviral particles were produced via transient transfection of the ecotropic Phoenix packaging cell line with the following plasmids: pWZL-hygro; pBABE-puro; pWZL-hygro 12S *E1A* or pBABE-puro *K-Ras* V12 (purchased from Addgene, Cambridge, MA). Primary WT or *Hsp70*$^{-/-}$ MEFs were plated in 6 well plates (4×10^4 - 2×10^5/well) and the next day 1ml of the appropriate retrovirus containing supernatants plus 8μg/ml polybrene added for approximately 6 hours. The viral supernatants were then removed and fresh medium added before allowing the cells to grow for an additional two days. Cells were then harvested and re-plated (2×10^5/well) in 6 well plates and antibiotic selection added (hygromycin (40μg/ml) and/or puromycin (0.5μg/ml)). After approximately 14 days colony outgrowth was visualized by methylene blue staining.

In some experiments, transformed MEFs were maintained in culture for experimentation – the genotype was confirmed by qPCR and these cell lines were maintained *in vitro* in DMEM, 10% FBS, 2mM non-essential amino acids, 100U/ml penicillin/streptomycin, 2mM glutamine and 0.5% β-mercaptoethanol for a maximum of 10 passages before retrieval of an earlier passage from liquid nitrogen storage. All cell lines generated were tested approximately every 3 months for mycoplasma contamination using MycoSEQ™ Mycoplasma Detection Assay (In Vitrogen) and discarded if found to be positive.

In Vitro Transformation of MEFs

Retroviral particles were produced using the ecotropic Phoenix packaging cell line with the following plasmids: pWZL-hygro; pBABE-puro; pWZL-hygro 12S *E1A* or pBABE-puro *K-Ras* V12 (purchased from Addgene, Cambridge, MA). Primary WT or *Hsp70*$^{-/-}$ MEFs were infected with virus for 6h before medium replacement, antibiotic selection and colony outgrowth visualized by methylene blue staining.

MEF Tumor Implantation

4.2×10^6 WT or *Hsp70*$^{-/-}$ *E1A/Ras* MEF transformants were introduced subcutaneously into each of the flanks of CD1-*Foxn1*^{nu}, C57BL/6J or *Hsp70*$^{-/-}$ as indicated in each figure mice and tumor growth monitored approximately every three days via ultrasound imaging. High-resolution data sets were acquired (at 25–40 MHz) in the coronal plane allowing for 3-D reconstruction using a VEVO-770 high-resolution ultrasound system (VisualSonics Inc., Toronto, Canada). Tumor volumes (mm^3) were calculated using the VEVO-770 software (version 3.0.0) and once tumor volume reached 20% of body mass, mice were euthanized and tumor tissue harvested for subsequent analyses. In some experiments blood, lymph nodes and spleens were also collected for subsequent cell isolation and immunophenotyping.

Cell Isolation and Immunophenotyping

Where indicated, spleen, lymph node or blood were collected from tumor burdened mice and subjected to immunophenotyping and FACS analysis as follows: ***Stain 1:*** CD3, APC (1:200); CD4-PerCpCy5 (1:200); CD25-FITC (1:50); FoxP3-PE (1:100); IL-2-PE-Cy7 (1:100) (blood, lymph nodes and spleen); ***Stain 2:*** CD3-Alexa 700 (1:200); DX5-FITC (1:50) or NK1.1-FITC (1:50); CD8-PerCp-Cy5 (1:100); CD4-PE-Cy7 (1:250); CD25-Pac Blue (1:50); IFNγ-APC (1:100); Granzyme B-PE (1:100); ***Stain 3:*** CD-11c-Pe-Cy7 (1:200); B220-APC-Cy7 (1:150); Gr-1-Pac Blue (1:100); CD-11b-Alexa 700 (1:100); CD25-FITC (1:50); IFNγ-APC (1:100); Granzyme B-PE (1:100). Antibodies were purchased from BD Biosciences, San Jose, CA or eBioscience, San Diego, CA. Samples were analyzed via flow cytometry and data analyzed using FloJo software.

Plasmids Used/Transfections/Transductions

WT *E1A/Ras* MEFs were transfected with pooled HuSH pRFP-c-RS shRNAs for *Hspa1a* and *Hspa1b* or the shRNA pRFP-c-RS negative control (all purchased from OriGene, Rockville, MD) using calcium phosphate (Invitrogen). Cells were cultured and sorted periodically until stable expression of RFP was confirmed. A retroviral vector encoding

p185 Bcr-Abl and GFP (MSCV-IRES-GFP) was used to generate retroviral particles by transfection of Phoenix-Eco cells (Invitrogen).

RNA isolation and qPCR

Total RNA was isolated using Trizol™ according to manufacturers instructions (Invitrogen, Carlsbad, CA), cDNA generated via reverse transcription and quantitative PCR performed using a 7900HT Fast Real time PCR system (Applied Biosystems, Foster City, CA) with 2μl cDNA in triplicate in a 25μl volume containing 50nM primers and appropriate volume of 5X Sybr Green PCR Master Mix (ABI). Primers used were: *Hsp70:* 5'-3' GGTGGTGCAGTCCGACAT (forward), 5'-3' TTGGGCTTGTCGCCGT (reverse); *Hsp90AA1*: 5'-3' AGACCCAAGACCAACCAATG (forward), 5'-3' AATCCGTTACGAGAGCCTGA (reverse), *Hsc70*: 5'-3' ATTTGTGTGGTCTCGTCGTC (forward), 5'-3' GTCCGTGAAAGCAACATAGC (reverse) and *L32*: 5'-3' GAAACTGGCGGAAACCCA (forward), 5'-3' GGATCTGGCCCTTGAACCTT (reverse).

Histopathology and Immunohistochemistry

Recovered tumors were initially fixed in 4% PFA overnight. Those used for paraffin sections were transferred to 10% neutral buffered formalin and embedded in paraffin wax, 4μM sections were prepared, stained with H&E and examined microscopically. Tumors used for cryosections were washed with PBS after overnight fixation and placed in 30% sucrose at 4°C until penetration was complete. The tumors were then placed in OCT embedding compound and 10μM sections prepared. Sections were then stained for HSP70 (C92) (Enzo Life Sciences, Farmingdale, NY), PECAM-1 (MEC13.3) (BD Biosciences), DAPI, MAC-2, F4/80, CD68, arginase 1, 7/4 (Abcam, Cambridge, MA) (neutrophil-specific), major basic protein (MBP) (eosinophil-specific), CD3 (Santa Cruz Biotechnology, Santa Cruz, CA), FoxP3 (T_{regs}), CD4 (H129.19) (BD Biosciences), CD8 (53.6.7) (eBioscience), NK1.1 (NK and NKT cells) (PK136) (eBioscience), CD-11b (Abcam), Gr-1 (eBioscience), perforin and granzyme B (polyclonal) (Abcam).

Analysis—Quantification of MAC-2 staining in tumors collected from CD1-*Foxn1*^{nu} hosts was evaluated using an Aperio slide scanner and the 'positive pixel count' algorithm that evaluates each pixel and assigns an arbitrary strongly positive, moderately positive, weakly positive, and negative staining to each. To determine the total MAC-2 positive area of tumors harvested from the CD1-*Foxn1*^{nu} mice, (= 'percent positivity') the number of strongly and moderately positive pixels was quantified in 10 randomly selected areas of 1mm^2 each (total area sampled = 10 mm^2) in sections from each WT and *Hsp70*$^{-/-}$ tumor.

Confocal Images

Confocal images were taken using a Zeiss LSM 510 NLO Meta point scanning confocal/ multiphoton microscope and Zen software.

Immunoblot

WT *E1A/Ras* MEFs stably expressing *Hspa1a/Hspa1b* or negative control RFP-shRNAs were subjected to heat shock for one hour at 42°C before recovery at 37°C for two hours.

Cells were harvested by centrifugation and lysed using 1X RIPA Buffer (Pierce Biotechnology Inc, Rockford, IL) containing protease inhibitor cocktail (Roche Applied Science, Indianapolis, IN). The extracts (20 μg total protein) were subjected to sodium dodecyl sulfate polyacrylamide gel electrophoresis (SDS-PAGE) on a 4–12% acrylamide gel before transfer to a nitrocellulose membrane. After blocking in 5% non-fat milk in TBS-Tween, blots were incubated with HSP70/HSP72 (1:1000; Enzo Life Sciences), RFP (1:2000; Origene) and actin (1:400; MP Biomedicals, Solon, OH) antibodies overnight at 4°C. Blots were then incubated for 30 minutes at room temperature with anti-mouse horseradish peroxidase conjugated secondary antibody (1:3000; Pierce Biotechnology, Inc). ECL or Supersignal West Femto Chemiluminescent Substrate (Pierce Biotechnology Inc) was used to visualize antigen-specific signals that were then imaged using Carestream 4000MM ImagePro image station and software.

Culture of *Bcr-Abl*-Transduced Bone Marrow

Procedures were performed as described previously (Williams et al. 2006). In brief, bone marrow was isolated from the femurs of WT or *Hsp70*$^{-/-}$ C57BL/6J mice and transduced with *Bcr-Abl-GFP* by adding a ratio of 1ml virus: 6×10^6 cells plus polybrene (8μg/ml) and incubated for 3h at 37°C. *In vitro culture:* Cells were washed and replated (10^6/ml) in RPMI medium (Biowhittaker, VWR, Radnor, PA) supplemented with 5% fetal calf serum (HyClone, Thermo Fisher Scientific, Waltham, MA), 4mM glutamine (Invitrogen) penicillin/streptomycin (Invitrogen) and 55μm β-mercaptoethanol (Gibco). Cultures were maintained in culture and cell growth and viability monitored for approximately 7 days, after which established cultures were transferred to maintenance medium (at 2×10^5/ml) (as above with 10% fetal calf serum). After approximately one week, cells were harvested for GFP assessment via flow cytometry and genotype confirmation by real-time PCR. *In vivo:* Transduced bone marrow (10^6/recipient) was introduced via *iv* into lethally irradiated (11Gy in two fractions) WT recipients maintained on antibiotic containing water. Mice were observed daily, monitored for signs of disease onset and sacrificed when exhibiting signs of distress. Lymphoid organs were harvested for subsequent analysis.

Eμ-Myc Model of Lymphomagenesis

Cohorts of *Eμ-Myc* mice, WT, heterozygous and null for *Hsp70* were monitored for onset of disease (average for WT mice is approximately 100 days) (Adams et al. 1985) and sacrificed once animals were deemed moribund. Lymphoid organs were harvested for subsequent analysis via immunostaining and flow cytometric analysis.

Migration Assays

Migration assays were conducted using the ChemoTx system (Neuro Probe, Inc., Gaithersburg, MD). Sizes of wells, filter and pores used were 300μl, 5.7mm, and 8μm respectively. 1.5×10^6 total splenocytes isolated from mice inoculated with WT or *Hsp70*$^{-/-}$ *E1A/Ras* MEF transformants 5 days prior, were introduced into the upper chamber of the culture well above 2000, 1000 or 500 WT or *Hsp70*$^{-/-}$ MEF transformants, cultured overnight at 37°C. Following a 4 hour incubation at 37°C, the number of cells migrated to

the lower well was enumerated using a Scepter cell counter (EMD Millipore, Billerica, MA).

Antigen Cross Presentation

Bone marrow was harvested from femurs and tibias of C57BL/6 *Hsp70.1/.3*$^{-/-}$ or WT littermates using a bone marrow harvesting and hematopoietic stem cell isolation kit (Millipore). Cells were plated into 15cm bacterial petri dishes (5×10^6/dish) containing 15ml of DC media (RPMI 1640 supplemented with 10% heat-inactivated FCS, 2mM L-glutamine, 100U/ml penicillin/100ug/ml streptomycin, 1mM sodium pyruvate, and 100μM nonessential amino acids) containing 20ng/ml recombinant murine GM-CSF (Peprotech, Rocky Hill, NJ). On day 3 an additional 15ml of DC medium was added to the cultures and after 6 days in culture 15ml of media was removed and replaced with fresh DC culture medium. On day 7 (12 hours before use in antigen presentation assays) non-adherent cells were harvested and enriched using the mouse dendritic cell enrichment set-DM (BD Bioscience, San Jose, CA) according to the manufacturer's instructions. Enriched DCs were routinely >85–95% $CD11c^+$ as determined by flow cytometry using an anti-CD11c antibody (clone N418).

OT-I (H-$2K_b$ restricted anti-OVA (257–264)) T cells were harvested from the pooled lymph nodes and spleens of OT-I transgenic mice. Single cell suspensions were generated before negative selection using CD8 (Miltenyi, Auburn, CA). Enriched cell preparations were >90% T cells as determined by flow cytometry using an antibody specific for CD8.

Enriched DCs (10^5) were plated in 96-well U-bottom plates and cultured overnight at 37°C in DC medium without GM-CSF. The next day cells were washed and fresh medium added containing Class I OVA peptide 257–264 (100μM). The next day dendritic cells were washed twice in HBSS and 1×10^5 OT-I transgenic T cells added to the wells. After approximately 72h cells were counted, using trypan blue to assess viability.

Statistical Analysis

Statistical significance was determined according to the test described in the relevant figure legend.

Supplementary Material

Refer to Web version on PubMed Central for supplementary material.

ACKNOWLEDGEMENTS

The authors wish to thank Dr Douglas Green for discussion during the preparation of this manuscript and to Eleanora Puetz and Alex Yu for genotyping. Special thanks to the husbandry staff of the Animal Resource Center and to the Animal Imaging Center including Christopher Calabrese, Melissa Johnson and Monique Payton. We are grateful to the flow cytometry facility for their assistance in FACS and flow analysis. This work was funded in part by core funding and Cancer Center Supporting Grant (CCSG) developmental funds (5P30CA021765–29) (to H.M.B.) and the American Lebanese-Syrian Associated Charities of St. Jude Children's Research Hospital.

REFERENCES

Adams JM, Harris AW, Pinkert CA, Corcoran LM, Alexander WS, Cory S, et al. The c-myc oncogene driven by immunoglobulin enhancers induces lymphoid malignancy in transgenic mice. Nature. 1985; 318:533–538. [PubMed: 3906410]

Asea A, Kraeft SK, Kurt-Jones EA, Stevenson MA, Chen LB, Finberg RW, et al. HSP70 stimulates cytokine production through a CD14-dependant pathway, demonstrating its dual role as a chaperone and cytokine. Nat Med. 2000; 6:435–442. [PubMed: 10742151]

Binder RJ, Srivastava PK. Peptides chaperoned by heat-shock proteins are a necessary and sufficient source of antigen in the cross-priming of CD8+ T cells. Nat Immunol. 2005; 6:593–599. [PubMed: 15864309]

Blachere NE, Li Z, Chandawarkar RY, Suto R, Jaikaria NS, Basu S, et al. Heat shock protein-peptide complexes, reconstituted in vitro, elicit peptide-specific cytotoxic T lymphocyte response and tumor immunity. J Exp Med. 1997; 186:1315–1322. [PubMed: 9334371]

Borges TJ, Wieten L, van Herwijnen MJ, Broere F, van der Zee R, Bonorino C, et al. The anti-inflammatory mechanisms of Hsp70. Front Immunol. 2012; 3:95. [PubMed: 22566973]

Chalmin F, Ladoire S, Mignot G, Vincent J, Bruchard M, Remy-Martin JP, et al. Membrane-associated Hsp72 from tumor-derived exosomes mediates STAT3-dependent immunosuppressive function of mouse and human myeloid-derived suppressor cells. J Clin Invest. 2010; 120:457–471. [PubMed: 20093776]

Chen T, Guo J, Han C, Yang M, Cao X. Heat shock protein 70, released from heat-stressed tumor cells, initiates antitumor immunity by inducing tumor cell chemokine production and activating dendritic cells via TLR4 pathway. J Immunol. 2009; 182:1449–1459. [PubMed: 19155492]

Ciocca DR, Arrigo AP, Calderwood SK. Heat shock proteins and heat shock factor 1 in carcinogenesis and tumor development: an update. Arch Toxicol. 2013; 87:19–48. [PubMed: 22885793]

Dai C, Whitesell L, Rogers AB, Lindquist S. Heat shock factor 1 is a powerful multifaceted modifier of carcinogenesis. Cell. 2007; 130:1005–1018. [PubMed: 17889646]

Daniels GA, Sanchez-Perez L, Diaz RM, Kottke T, Thompson J, Lai M, et al. A simple method to cure established tumors by inflammatory killing of normal cells. Nat Biotechnol. 2004; 22:1125–1132. [PubMed: 15300260]

Dunn GP, Old LJ, Schreiber RD. The three Es of cancer immunoediting. Annu Rev Immunol. 2004; 22:329–360. [PubMed: 15032581]

DuPage M, Mazumdar C, Schmidt LM, Cheung AF, Jacks T. Expression of tumour-specific antigens underlies cancer immunoediting. Nature. 2012; 482:405–409. [PubMed: 22318517]

Effendi K, Sakamoto M. Molecular pathology in early hepatocarcinogenesis. Oncology. 2010; 78:157–160. [PubMed: 20389138]

Elsner L, Muppala V, Gehrmann M, Lozano J, Malzahn D, Bickeboller H, et al. The heat shock protein HSP70 promotes mouse NK cell activity against tumors that express inducible NKG2D ligands. J Immunol. 2007; 179:5523–5533. [PubMed: 17911639]

Gross C, Hansch D, Gastpar R, Multhoff G. Interaction of heat shock protein 70 peptide with NK cells involves the NK receptor CD94. Biol Chem. 2003; 384:267–279. [PubMed: 12675520]

Hunt CR, Dix DJ, Sharma GG, Pandita RK, Gupta A, Funk M, et al. Genomic instability and enhanced radiosensitivity in Hsp70.1- and Hsp70.3-deficient mice. Mol Cell Biol. 2004; 24:899–911. [PubMed: 14701760]

Kottke T, Pulido J, Thompson J, Sanchez-Perez L, Chong H, Calderwood SK, et al. Antitumor immunity can be uncoupled from autoimmunity following heat shock protein 70-mediated inflammatory killing of normal pancreas. Cancer Res. 2009; 69:7767–7774. [PubMed: 19738045]

Leu JI, Pimkina J, Frank A, Murphy ME, George DL. A small molecule inhibitor of inducible heat shock protein 70. Mol Cell. 2009; 36:15–27. [PubMed: 19818706]

Li Z, Menoret A, Srivastava P. Roles of heat-shock proteins in antigen presentation and cross-presentation. Curr Opin Immunol. 2002; 14:45–51. [PubMed: 11790532]

Malusecka E, Krzyzowska-Gruca S, Gawrychowski J, Fiszer-Kierzkowska A, Kolosza Z, Krawczyk Z. Stress proteins HSP27 and HSP70i predict survival in non-small cell lung carcinoma. Anticancer Res. 2008; 28:501–506. [PubMed: 18383892]

Mambula SS, Calderwood SK. Heat shock protein 70 is secreted from tumor cells by a nonclassical pathway involving lysosomal endosomes. J Immunol. 2006; 177:7849–7857. [PubMed: 17114456]

Matzinger P. Tolerance, danger, and the extended family. Annu Rev Immunol. 1994; 12:991–1045. [PubMed: 8011301]

Millar DG, Garza KM, Odermatt B, Elford AR, Ono N, Li Z, et al. Hsp70 promotes antigen-presenting cell function and converts T-cell tolerance to autoimmunity in vivo. Nat Med. 2003; 9:1469–1476. [PubMed: 14625545]

Min JN, Huang L, Zimonjic DB, Moskophidis D, Mivechi NF. Selective suppression of lymphomas by functional loss of Hsf1 in a p53-deficient mouse model for spontaneous tumors. Oncogene. 2007; 26:5086–5097. [PubMed: 17310987]

Multhoff G. Activation of natural killer cells by heat shock protein 70. Int J Hyperthermia. 2002; 18:576–585. [PubMed: 12537756]

Nylandsted J, Rohde M, Brand K, Bastholm L, Elling F, Jaattela M. Selective depletion of heat shock protein 70 (Hsp70) activates a tumor-specific death program that is independent of caspases and bypasses Bcl-2. Proc Natl Acad Sci U S A. 2000; 97:7871–7876. [PubMed: 10884417]

Rohde M, Daugaard M, Jensen MH, Helin K, Nylandsted J, Jaattela M. Members of the heat-shock protein 70 family promote cancer cell growth by distinct mechanisms. Genes Dev. 2005; 19:570–582. [PubMed: 15741319]

Srivastava P. Interaction of heat shock proteins with peptides and antigen presenting cells: chaperoning of the innate and adaptive immune responses. Annu Rev Immunol. 2002a; 20:395–425. [PubMed: 11861608]

Srivastava P. Roles of heat-shock proteins in innate and adaptive immunity. Nat Rev Immunol. 2002b; 2:185–194. [PubMed: 11913069]

Stocki P, Dickinson AM. The immunosuppressive activity of heat shock protein 70. Autoimmune Dis. 2012; 2012:617213. [PubMed: 23326648]

Stocki P, Wang XN, Dickinson AM. Inducible heat shock protein 70 reduces T cell responses and stimulatory capacity of monocyte-derived dendritic cells. J Biol Chem. 2012; 287:12387–12394. [PubMed: 22334699]

Torronteguy C, Frasson A, Zerwes F, Winnikov E, da Silva VD, Menoret A, et al. Inducible heat shock protein 70 expression as a potential predictive marker of metastasis in breast tumors. Cell Stress Chaperones. 2006; 11:34–43. [PubMed: 16572727]

Udono H, Srivastava PK. Heat shock protein 70-associated peptides elicit specific cancer immunity. J Exp Med. 1993; 178:1391–1396. [PubMed: 8376942]

van Eden W, Spiering R, Broere F, van der Zee R. A case of mistaken identity: HSPs are no DAMPs but DAMPERs. Cell Stress Chaperones. 2012; 17:281–292. [PubMed: 22139593]

van Herwijnen MJ, Wieten L, van der Zee R, van Kooten PJ, Wagenaar-Hilbers JP, Hoek A, et al. Regulatory T cells that recognize a ubiquitous stress-inducible self-antigen are long-lived suppressors of autoimmune arthritis. Proc Natl Acad Sci U S A. 2012; 109:14134–14139. [PubMed: 22891339]

Vega VL, Rodriguez-Silva M, Frey T, Gehrmann M, Diaz JC, Steinem C, et al. Hsp70 translocates into the plasma membrane after stress and is released into the extracellular environment in a membrane-associated form that activates macrophages. J Immunol. 2008; 180:4299–4307. [PubMed: 18322243]

Wachstein J, Tischer S, Figueiredo C, Limbourg A, Falk C, Immenschuh S, et al. HSP70 enhances immunosuppressive function of CD4(+)CD25(+)FoxP3(+) T regulatory cells and cytotoxicity in CD4(+)CD25(−) T cells. PLoS One. 2012; 7:e51747. [PubMed: 23300563]

Williams RT, Roussel MF, Sherr CJ. Arf gene loss enhances oncogenicity and limits imatinib response in mouse models of Bcr-Abl-induced acute lymphoblastic leukemia. Proc Natl Acad Sci U S A. 2006; 103:6688–6693. [PubMed: 16618932]

Zietara N, Lyszkiewicz M, Gekara N, Puchalka J, Dos Santos VA, Hunt CR, et al. Absence of IFN-beta impairs antigen presentation capacity of splenic dendritic cells via down-regulation of heat shock protein 70. J Immunol. 2009; 183:1099–1109. [PubMed: 19581626]

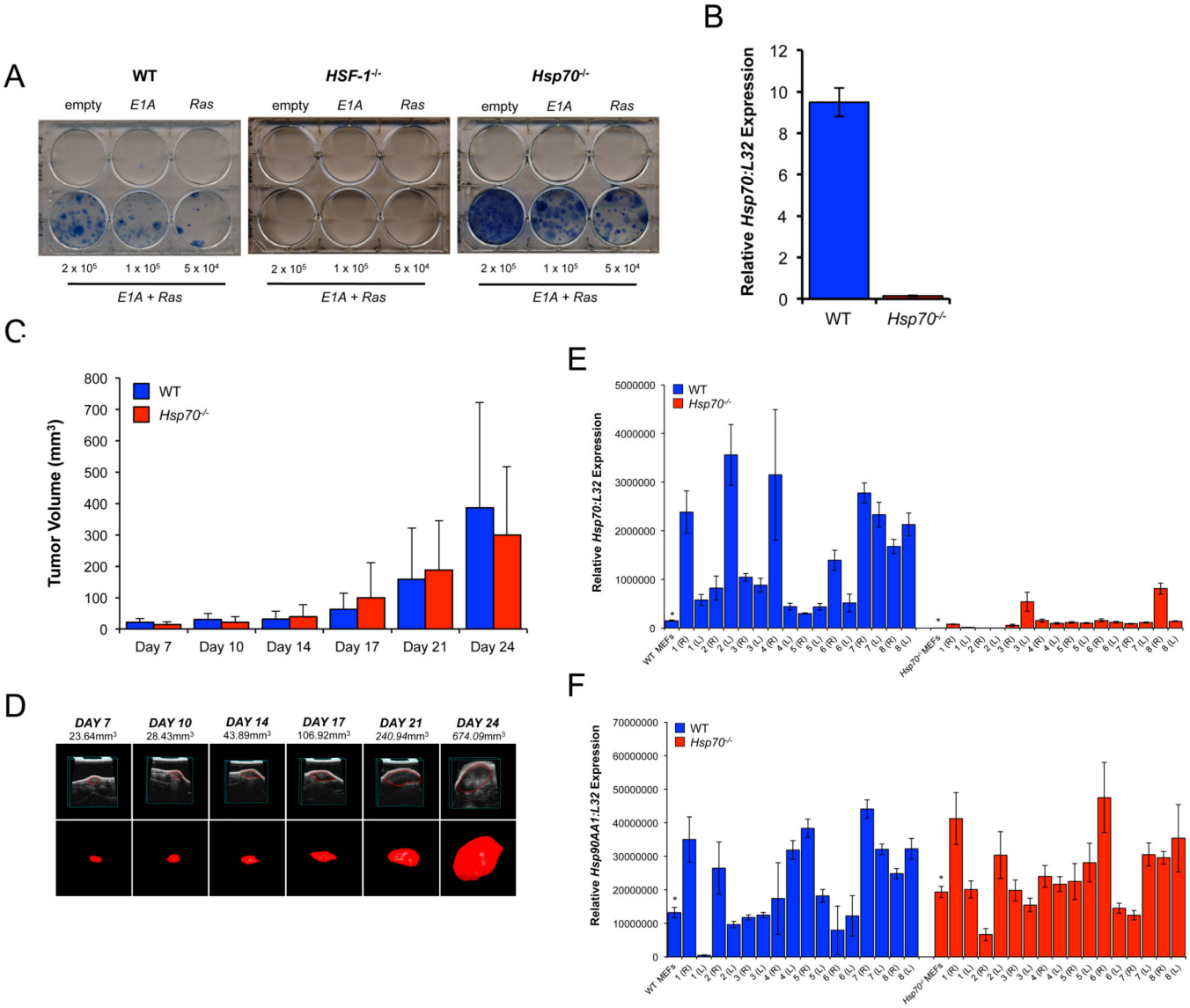

Figure 1. *Hsp70* is Neither Required for *in vitro* Transformation nor Tumor Growth *in* vivo

WT, *HSF-1*$^{-/-}$ or *Hsp70*$^{-/-}$ primary MEFs were transduced with empty vector control, *E1A* or *Ras* alone or both *E1A and Ras* retroviral vectors as indicated and after re-plating (4×10^4 - 2×10^5/well) and antiobiotic selection for approximately 14 days, colonies were visualized by methylene blue staining **(A)**. qPCR for *Hsp70* (normalized to *L32* expression) of emergent colonies **(B)**. WT or *Hsp70*$^{-/-}$ *E1A/Ras* transformants were injected subcutaneously into each of the flanks of CD1-*Foxn1*^{nu} mice and tumor growth monitored by ultrasound. Volumetric tumor measurements (mm^3) were derived from 3-D reconstructions of the ultrasound datasets. Data is shown as the average (n = 5–10 mice/group) +/− SD and is representative of six independent experiments **(C)**. Representative images of one tumor (marked with * in **(C)**) in which the left panels show 2-D slices of the tumor and the right panels show the 3-D volumetric reconstruction **(D)**. Relative expression of *Hsp70* **(E)** and *Hsp90AA1* **(F)** normalized to *L32*. Asterisks denote the expression levels of *Hsp70* and *Hsp90AA1* in the MEFs used for inoculation.

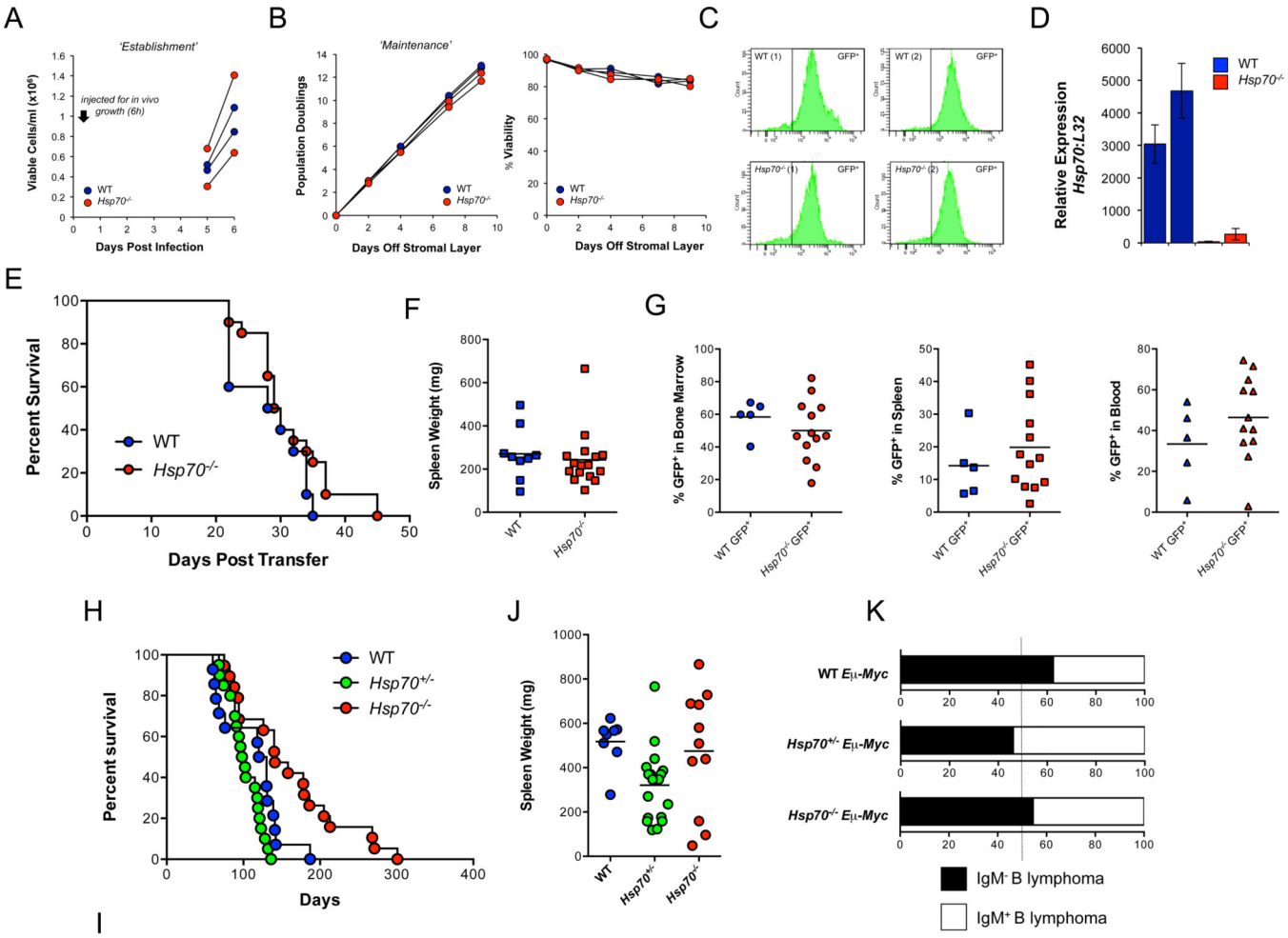

I

SURVIVAL CURVE ANALYSIS (Log Rank Mantel Cox)			MEDIAN SURVIVAL (Days)		
WT vs Hsp70+/-	WT vs Hsp70-/-	Hsp70+/- vs Hsp70-/-	WT	Hsp70+/-	Hsp70-/-
NS	*p=0.0173	***p=0.0003	125	100	141

Figure 2. Neither *Bcr-Abl* nor Eμ-Myc Requires HSP70 to induce Lymphoma

Bone marrow from each of two WT and two *Hsp70*$^{-/-}$ mice was transduced with a retroviral vector expressing *Bcr-Abl-GFP*. Cell growth was monitored before **(A)** and after cells were removed from the stromal layer **(B)**. After approximately 2 weeks GFP expression was assessed via flow cytomtery (**C)** and *Hsp70* gene expression via qPCR **(D)**. Survival of the two cohorts receiving *Bcr-Abl-GFP* transduced WT or *Hsp70*$^{-/-}$ bone marrow **(E)**, spleen weight **(F)** and % GFP^{+} cells in the bone marrow, spleen and blood **(G)**. Lymphoma free survival of WT, *Hsp70*$^{+/-}$ and *Hsp70*$^{-/-}$ Eμ-*Myc* mice **(H)** and average spleen weight **(J)**. Statistical evaluation of lymphoma free survival using a Log Rank Mantel Cox test (Prism Software) and median survival (in days) **(I)**. Relative frequencies (expressed as a percentage) of IgM^{-} pre B cell lymphomas and IgM^{+} mature B cell lymphomas as determined by the % IgM staining of the B220^{+} population in the spleen (<50% IgM^{+} was assigned a pre B phenotype) **(K)**.

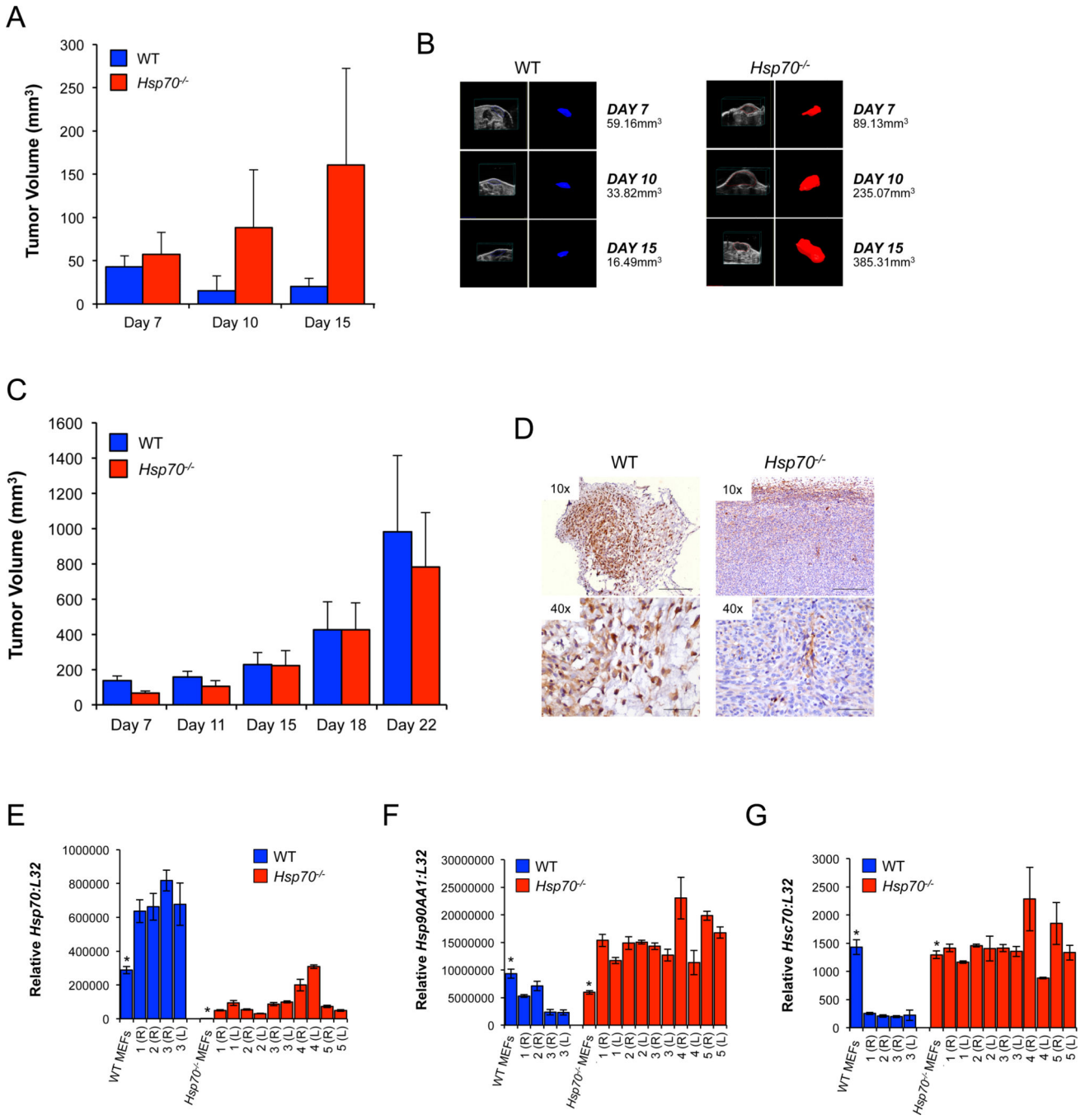

Figure 3. Growth of WT and *Hsp70*$^{-/-}$ Tumors is Dependent on the Immune Status of the Host

WT or *Hsp70*$^{-/-}$ *E1A/Ras* MEF transformants were injected subcutaneously into each of the flanks of C57BL/6J **(A)** or CD1-*Foxn1*^{nu} **(C)** mice. Volumetric tumor measurements (mm^3) were derived from 3-D reconstructions of the ultrasound datasets (one representative tumor from each of the WT and *Hsp70*$^{-/-}$ groups is shown **(B)**). A total of 32 WT C57BL/6J mice (in three independent experiments) and 55 CD1-*Foxn1*^{nu} mice (in six independent experiments) were used to assess *in vivo* tumor growth. One representative C57BL/6J experiment is shown in **(A)** and for comparison, two independent CD1-*Foxn1*^{nu} experiments

are shown in **(C)** and Figure 1 **(C)**. HSP70 expression in tumors from C57BL/6J mice was determined via immunostaining **(D)**. The scale bars correspond to 250 or 50 microns in the 10× and 40× images respectively. RNA from the tumors was used to determine the expression of *Hsp70* **(E)**, *Hsp90AA1* **(F)** and *Hsc70* **(G)** via qPCR. Relative gene expression is shown and all data were normalized to the control gene *L32*. Left (L) and right (R) flank tumors are numbered sequentially and asterisks denote the expression levels in the transformants used for inoculation.

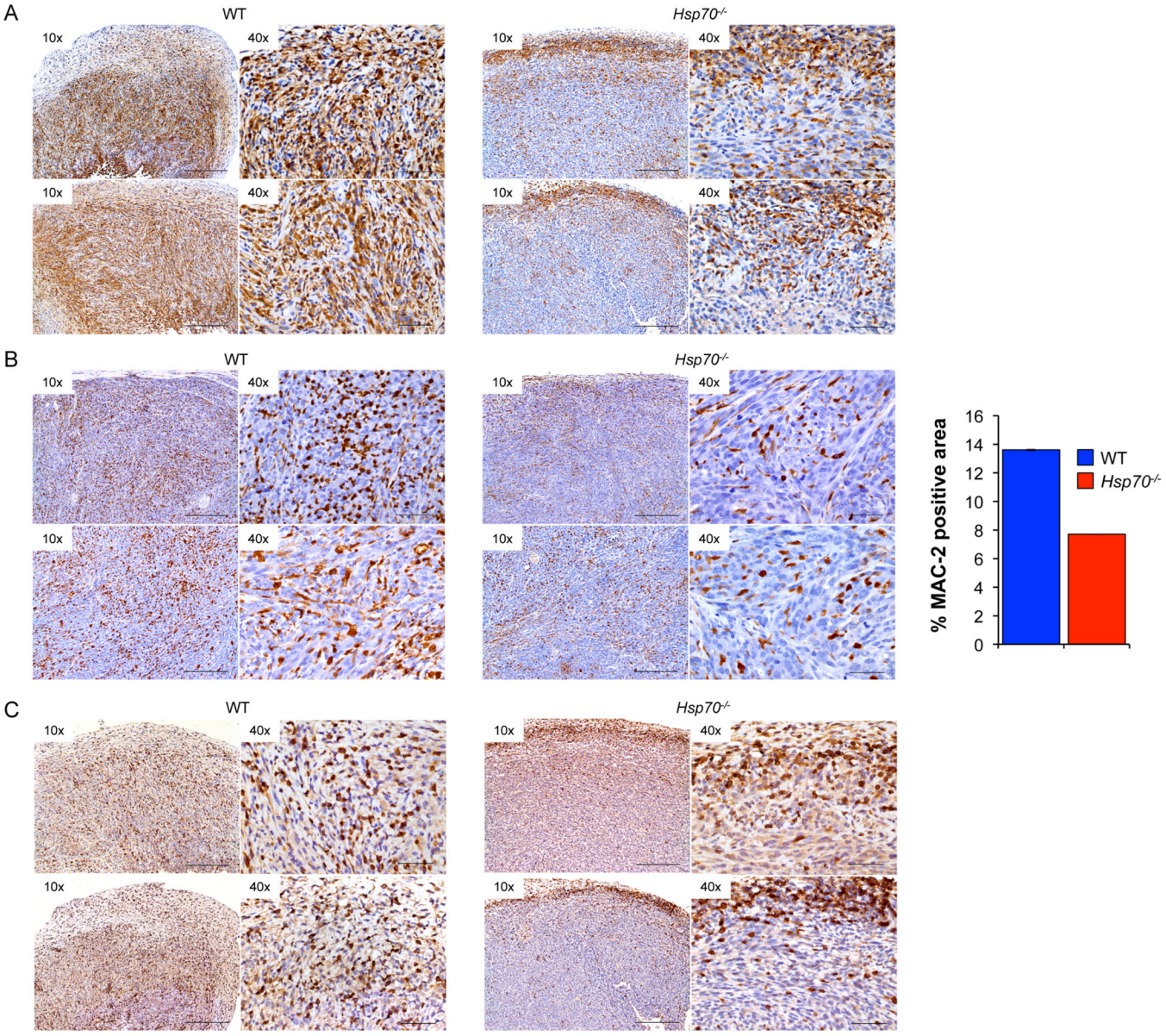

Figure 4. *Hsp70*$^{-/-}$ Tumors are Associated with a Significant Reduction in Immune Cell Infiltration

MAC-2 staining of tumors from C57BL/6J **(A)** or CD1-*Foxn1*^{nu} **(B)** hosts. Quantification of MAC-2 staining in tumors collected from CD1-*Foxn1*^{nu} hosts was evaluated and expressed as 'percent positivity'. CD3 staining of WT and *Hsp70*$^{-/-}$ tumors to visualize T cell distribution **(C)**. Images shown are representative from 2 WT and 2 *Hsp70*$^{-/-}$ tumors at the magnifications are shown. The scale bars correspond to 250 or 50 microns in the 10× and 40× images respectively.

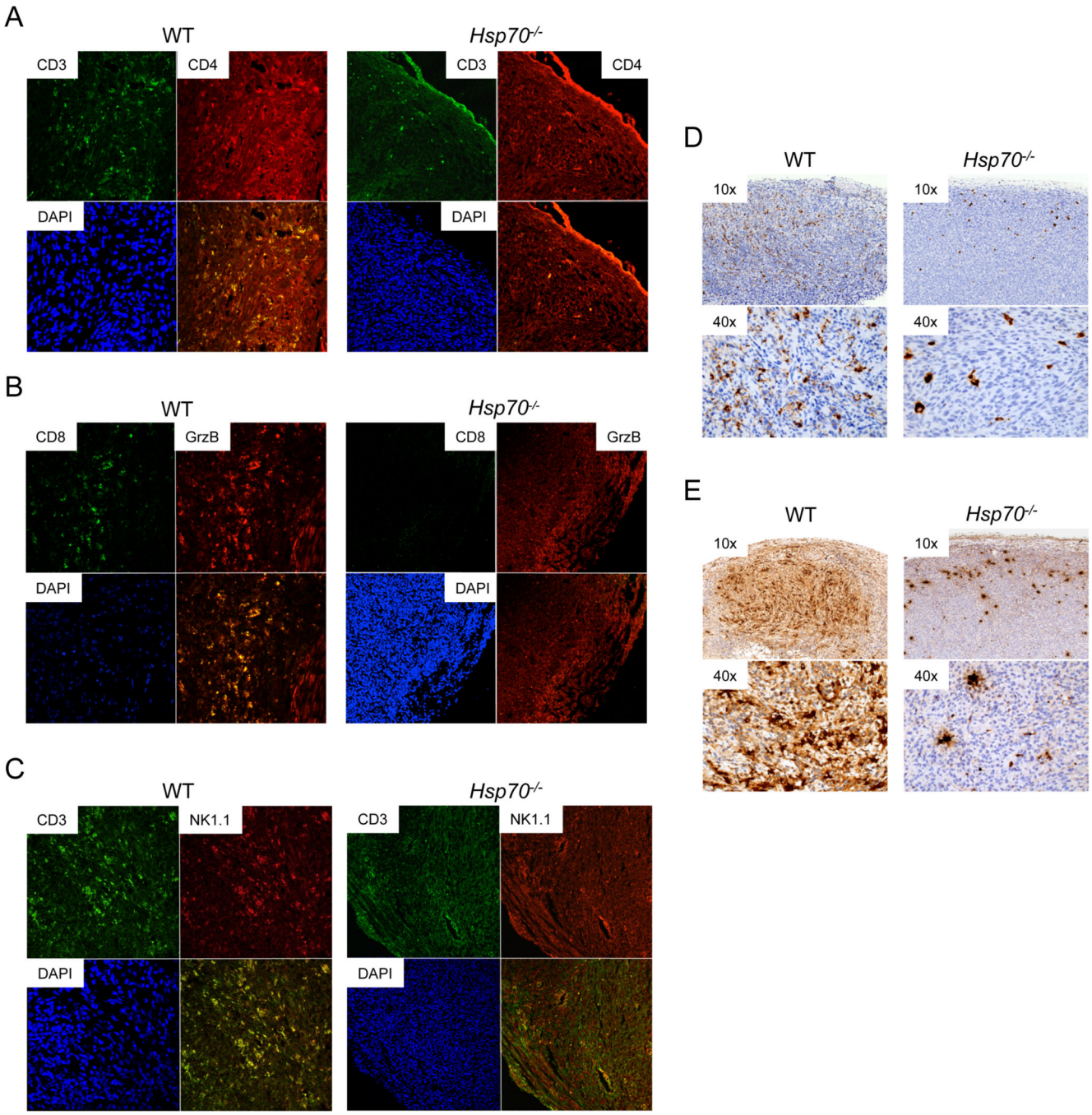

Figure 5. *Hsp70*$^{-/-}$ Tumors are Associated with a Significant Reduction in Immune Cell Infiltration

WT or *Hsp70*$^{-/-}$ tumors were processed for dual immunofluorescence using antibodies for CD3 (A4A88 = green) and CD4 (Cy-3 = red) **(A)**, CD8 (A4A88 = green) and granzyme B (GrzB) (Cy-3 = red) **(B)** or CD3 (A4A88 = green) and NK1.1 (Cy-3 = red) **(C)**. DAPI staining (blue) was used to visualize the nuclei and magnification of representative images shown is 20–40×. Representative images from one WT and one *Hsp70*$^{-/-}$ tumor are shown. Representative images from 1 WT and 1 *Hsp70*$^{-/-}$ tumor are included for granzyme B **(D)**

and perforin **(E)** and the magnifications are shown at the upper left hand corner of each panel.

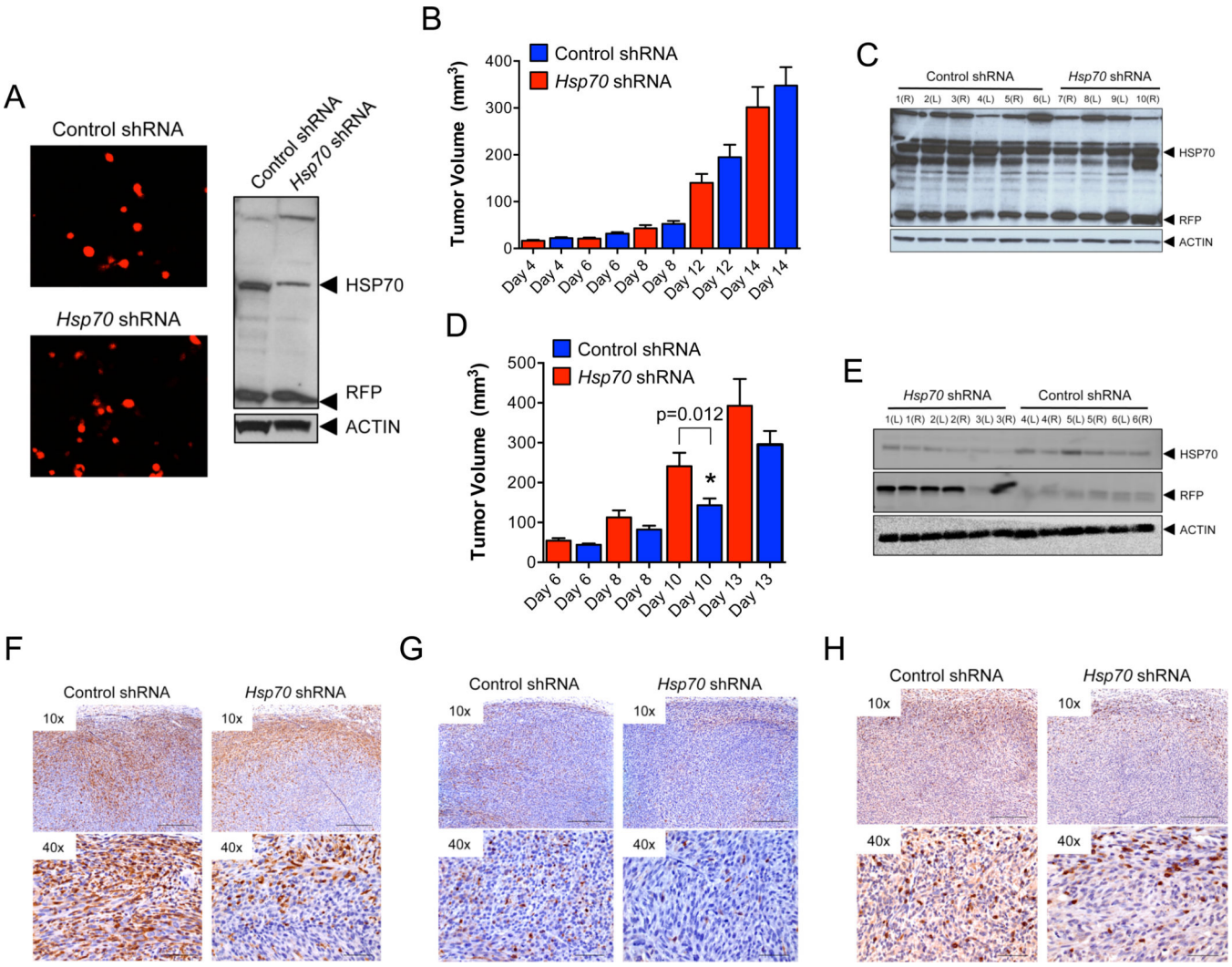

Figure 6. Tumor Growth *in vivo* Selects against HSP70 Expression in an Immune Competent Host

Immunoblot of WT transformants stably expressing RFP-vectors expressing *Hsp70* or control shRNAs for HSP70 and RFP expression **(A)** WT-*Hsp70*-shRNA or WT-control-shRNA tumor cells were injected subcutaneously into each of the flanks of CD1-*Foxn1*^{nu} **(B)** or C57BL/6J **(D)** mice and tumor volumes monitored by ultrasound. Each data point represents one tumor (n = 10 mice/group) and average tumor volume +/− SEM per time point is shown and p values were derived from one-way ANOVA analysis (Prism Software). Tumors were collected for immunoblotting for HSP70, RFP and actin (loading control). Representative blots are shown in **(C)** and **(E)** for tumors harvested from CD1-*Foxn1*^{nu} or C57BL/6 mice respectively. Tumors were processed for MAC2 **(F)** (C57BL/6J hosts) and **(G)** (CD1-*Foxn1*^{nu} hosts) or CD3 **(H)** immunostaining. Images of one representative tumor of each genotype (WT-*Hsp70*-shRNA or WT-control-shRNA) at the magnifications indicated are included. The scale bars correspond to 250 or 50 microns in the 10× and 40× images respectively.

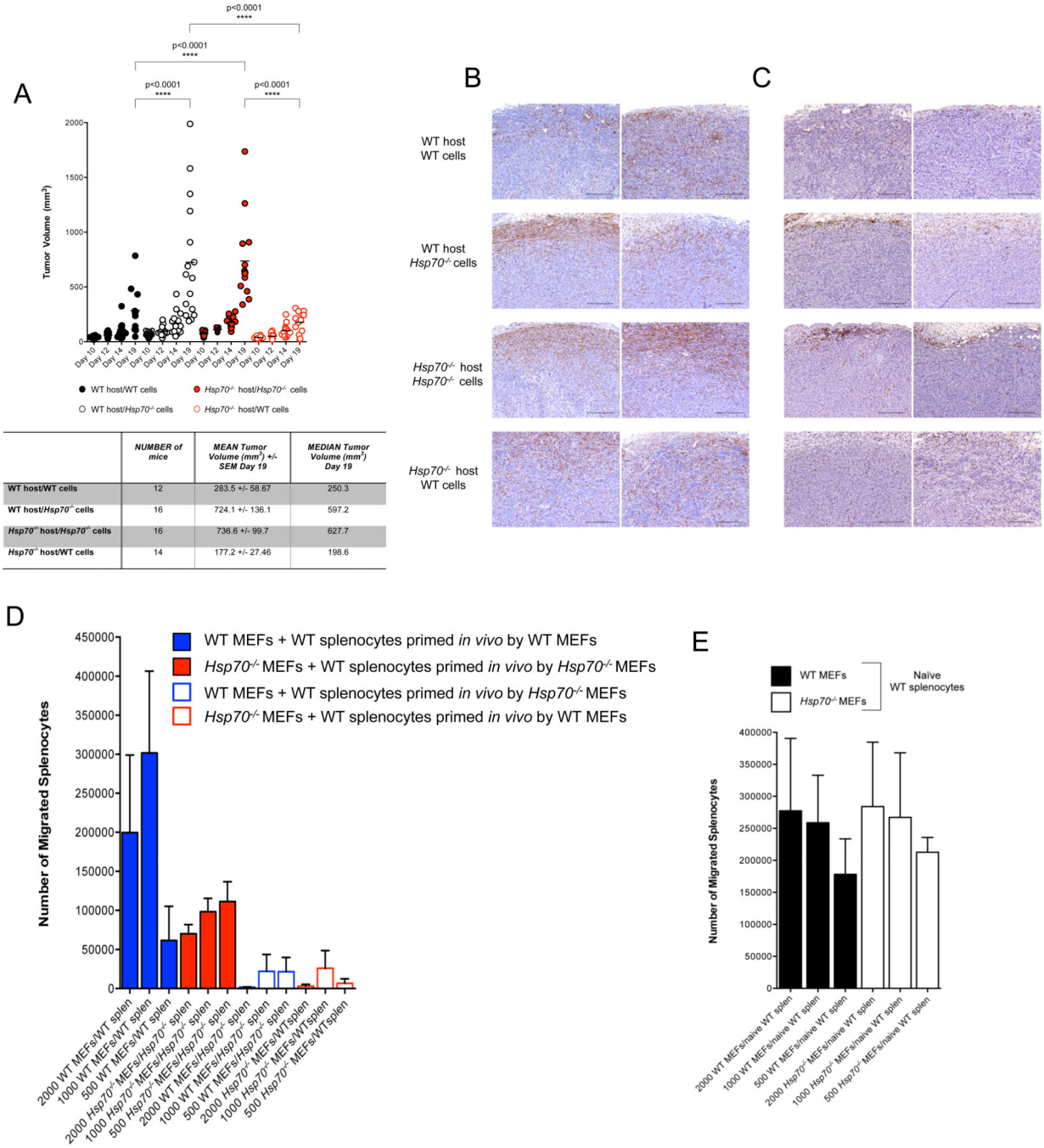

	NUMBER of mice	MEAN Tumor Volume (mm^3) +/- SEM Day 19	MEDIAN Tumor Volume (mm^3) Day 19
WT host/WT cells	12	283.5 +/- 58.67	250.3
WT host/*Hsp70*$^{-/-}$ cells	16	724.1 +/- 136.1	597.2
Hsp70$^{-/-}$ host/*Hsp70*$^{-/-}$ cells	16	736.6 +/- 99.7	627.7
Hsp70$^{-/-}$ host/WT cells	14	177.2 +/- 27.46	198.6

Figure 7. Tumor-Derived HSP70 Functions in a Chemokine-Like Manner to Facilitate Intra-Tumoral Infiltration of Immune Cells

WT or *Hsp70*$^{-/-}$ *E1A*/Ras transformants were injected bilaterally into WT and *Hsp70*$^{-/-}$ C57BL/6J mice and tumor growth monitored over approximately 3 weeks via ultrasound imaging **(A)**. Each data point represents a single tumor from two independent experiments and a summary of the data is shown in the table below. Statistical significance was determined via one-way ANOVA (Prism Software). Tumors were harvested and stained for MAC2 **(B)** or CD3 **(C)**. Migration assays were performed using splenocytes isolated from

WT C57BL/6J mice injected bilaterally with WT or *Hsp70*$^{-/-}$ MEFs 5 days prior **(D)** or non-challenged mice **(E)**. Each experiment shown is representative of three independent experiments conducted in triplicate.